CIMAC CONGRESS 25
ZURICH, MAY 19 – 23, 2025

2025 | 287

A methodology for data-driven diagnosis of marine two-stroke dual-fuel engines

Controls, Automation, Measurement, Monitoring & Predictive Maintenance

Ioannis Sklias, WinGD

Gerasimos Theotokatos, University of Strathclyde
Jaehan Jeon, University of Strathclyde

ABSTRACT

As maritime industry moves towards a carbon neutral future, ship systems are gradually becoming more sophisticated and complex. Apart from decarbonisation, digitalisation of those systems is crucial to improve their energy efficiency, enhance safety and reduce their environmental footprint. Data-driven diagnostics as well as prognostics and health management (PHM) digital tools are expected to contribute significantly to the safe and cost-effective operation of ships. The development of these tools requires datasets representing wide operating envelopes, which however, are not readily available in the shipping industry. This study aims to develop a novel health diagnosis methodology for two-stroke marine engines, with the objective to identify the engine components' health condition using acquired performance parameters. The methodology consists of the following three phases: (a) data correction and conditioning that employs advanced data analysis methods to remove noise and outliers from historical engine datasets leading to reference distributions of key performance parameters; (b) development and calibration of a physics-based digital twin by extending an existing thermodynamic model and incorporating the degradation patterns of selected engine components; this digital twin will then be employed to derive simulated datasets representing the engine operation across a wider range of conditions than covered by the available measurements. (c) development of data-driven models based on three methods; namely, artificial neural networks (NN) of multilayer perceptron (MLP) type and k-Nearest Neighbor (kNN) and support vector machines (SVM) which proved to be most effective in previous studies, to predict the health indicators of engine components. This data-driven model will be trained and validated based on the synthetic datasets, whereas it will be tested by providing as input non-supervised datasets. The proposed methodology will be demonstrated through case studies considering the fuel injector degradation of a marine two-stroke dual-fuel engine, for which extensive measured datasets are available. The expected results include the data-driven model layout to provide the highest accuracy. Proving this methodology's effectiveness will facilitate its implementation as part of a shipboard diagnosis system, as well as the development of prognostics and health management tools, which are required for smart/intelligent ship operation.

1 INTRODUCTION

The maritime industry has been developing and adopting sustainable measures to achieve decarbonisation and net-zero targets set by international and national organizations [1]. Ship manufacturers have already introduced low carbon fuels in the market, such as liquified natural gas (LNG), which offers a substantial reduction of CO_2 emissions [2]. In recent years, marine dual fuel engines have been extensively employed to decarbonize shipping operations. Alternative fuels engines could require readjustment of their maintenance strategies. The pertinent literature argues that marine dual fuel engines demonstrate similar reliability to conventional marine diesel engines [3]. Regardless of the fuel selection, decarbonization and sustainability targets lead ship operators and engine manufacturers to develop effective diagnostics and prognostics for marine engines.

Over the last years, the application of engine diagnostic measures is shifted into more data-driven approaches or hybrid methodologies, including physical models and machine learning or artificial intelligence techniques [4]. Actions from industrial original equipment manufacturers (OEMs) are already in place, such as WinGD's WiDE platform [5], which employs real-time field data, digital twins and machine learning to perform monitoring and diagnostic tasks.

With the introduction though of marine dual fuel engines, several new faults and issues have arisen during their operation compared to diesel engines. One of the notable faults pertains to the liquid fuel injectors, more specifically the clogging effect, where one or more holes of the injector nozzle are blocked, leading to a reduced flow area during injection [6]. This effect, as well as several new faulty conditions associated with the use of low and zero carbon fuels must be effectively addressed.

This study aims at developing a methodology for components faulty conditions isolation and diagnostics, by integrating measured data sets, physical models, as well as examining machine learning and data-driven methods. The study focuses on this degradation of clogging for liquid fuel injectors for marine dual fuel two-stroke engines, which is one of the most common faults according to the service reports [6]. The fuel injectors are especially susceptible to thermal and mechanical stresses when the engine operates in the gas and diesel modes, due to the high temperatures of the combustion products (in the former), and the liquid fuel high pressure (in the latter). Various conditions and combinations of these stresses impact the health of the injector nozzle. This study scope is to detect faulty injectors and identify the level of severity of their fault.

2 INVESTIGATED SYSTEM

The investigated marine dual fuel engine is used as the propulsion engine of an LNG carrier vessel. The main characteristics of the engine and vessel are listed in Table 1.

Table 1. Investigated engine basic characteristics.

	Value	Unit
Vessel type	LNG Carrier	-
Deployment year	2020	-
No. engines	2	-
Engine type	W5X72DF	-
Engine maker	WinGD	-
Rated power	11,350	kW
Rated speed	74	rpm
BMEP	14.65	bar
Main gas fuel	LNG	-
Main and Pilot liquid fuel	MDO	-
Liquid fuel injection type	Direct (High Pr.)	-
Liquid fuel inj. pressure	500-900	bar
Gas fuel injection type	Direct (Low Pr.)	-
Gas fuel inj. pressure	5-15	bar

Further information about the engine and more specific characteristics can be found by the engine designer sources [7].

Each engine cylinder has installed a number of main fuel injector bodies, with each injector body consisting of several nozzles to achieve effective fuel injection. Each nozzle target is to achieve ideal fuel distributions and atomization, which is required for the effective diffusive combustion [8]. Over time, the injector nozzles are subject to numerous faults, such as clogging by deposits accumulation or cracks, which would affect their performance [9]. The effects of these faulty conditions on the engine performance variables are investigated, as part of the developed methodology.

3 METHODOLOGY

The proposed methodology, illustrated on Figure 1, consists of the following three main phases:

Phase (A): data correction and conditioning. This phase focuses on identifying reference values for the engine key performance parameters in steady state conditions by employing advanced data analysis methods to remove erroneous data and outliers from historical and measured engine datasets.

Phase (B): customisation and calibration of the model for the investigated marine engine. This phase deals with extending an existing thermodynamic model and incorporating sub-models representing the degradation of liquid main fuel injectors. This model is subsequently employed to derive simulated datasets representing the engine operation across a wider range of conditions compared to the available measurements. These datasets are then fed as input in Phase (C).

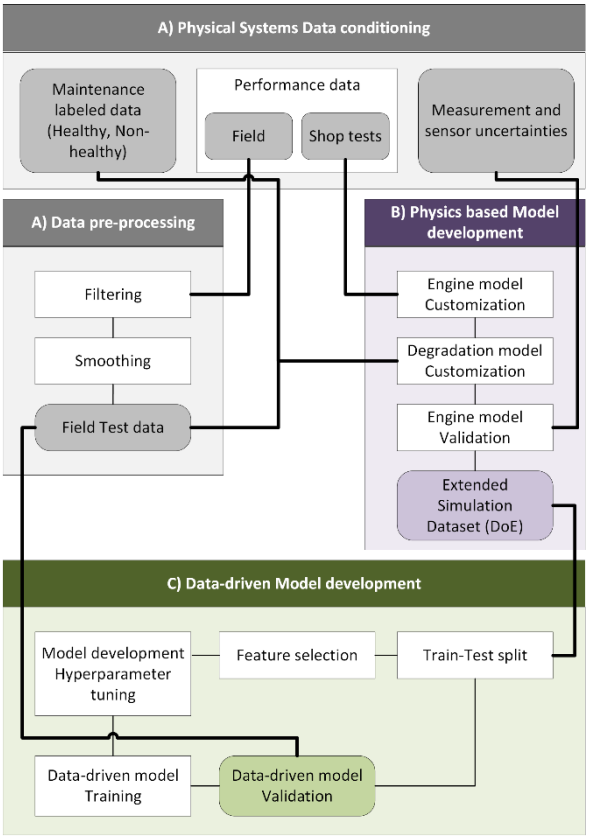

Figure 1. Data-driven diagnostic model development methodology flowchart.

Phase (C): development of data-driven (DD) models. This development is based on comparing three methods; namely, artificial neural networks (ANN) of the multilayer perceptron (MLP) type, Support Vector Machine (SVM), and k-Nearest Neighbor (KNN). Previous studies proved that MLP is the most effective to predict the health indicators of engine components [10]. However, SVM and KNN are also commonly used and easily set-up methods, which can be effective in several regression tasks [11], [12]. The developed data-driven models are trained and validated based on the extended datasets, whereas they will be tested by providing as input simulated and real testing datasets.

The proposed methodology is demonstrated through the case study of clogged main fuel injectors for the investigated marine dual-fuel two-stroke engine, for which considerable measured datasets from field measurements are available.

3.1 Physical systems data

The pool of the physical systems data consists of the following three dataset types:

1. Performance data (shop test and field measurements)
2. Maintenance parameters (healthy or non-healthy labels)
3. Sensor and measurement error margins / deviations

The largest portion of data pertains to the engine performance parameters. These data are typically measured during shop tests or in the operation field (onboard the ship). Shop tests are conducted for the approval of the engine performance, with the engine tested on a propeller curve conditions, setting the load by a brake. Shop tests usually result in acquiring the highest amount of recording datasets, as more instruments/sensors are employed to provide confidence on the approval process.

During field measurements, datasets for performance parameters are recorded while the vessel is operated, typically in a standard sampling rate of 1 min. The recorded raw datasets are fewer in number but higher in volume, compared the shop tests. For this study, the field data were acquired from WiDE, which is the integrated monitoring, diagnostic and digital expert system of WinGD [5].

Maintenance parameters mainly state the health of a component as fully healthy or non-healthy. This information is derived from the date of overhaul or replacement of the respective component, according to the Planned Maintenance System (PMS) of the vessel, as well as the maintenance activities reports from Chief engineers. Unofficial feedback from Chief Engineers is helpful, as additional information for the component condition/state can be obtained, such as failures, number of components, or failure type/severity. This information is used to define a Health Index for each component, which is subsequently to train the data-driven degradation models.

Errors of accuracy of sensor and measured parameters are used to define respective permissible deviation for the physics-based model

results. Table 2 lists all the recorded engine variables along with the respective measurement error according to the sensor technical specifications. This table also provides the availability of the recorded signal sensor in the field measurements. Nearly half of the signals are not recorded on field conditions, which could raise challenges for validating the physics-based model. The unavailability of field measured parameters is also associated with challenges to train and validate the data-driven models. This research gap is addressed herein by employing the derived simulation results from the physics-based model (or digital twin). However, the use of digital twins to provide virtual signals of non measured variables is out of this study scope.

Table 2. Acquired signals and error margins.

Signal	Sensor error (%)	ISO 15550 permissible deviation (%)	Field availability	Considered for model validation	Comment
Engine power (load)	n/a	3	Yes*	No	Setpoint
Engine speed	0.02	2	Yes	No	Input
Turbocharger Speed	0.02	2	Yes	Yes	-
Servo oil pressure	0.2	5	Yes	No	Not used
Main fuel rail pressure	0.2	10	Yes	No	Input
Pilot fuel rail pressure	0.2	10	Yes	No	Input
Temperature of main fuel	2	1.7	n/a	No	Input
Wastegate position	n/a	0	Yes	No	Not used
Ambient pressure	0.04	0.5	Yes	No	Input
Ambient temperature	2	0.7	Yes	No	Input
Relative humidity	2	0	n/a	No	Input
Air cooler pressure drop	2.5	10	n/a	Yes	-
Air filter pressure drop	2.5	5	n/a	Yes	-
Pressure after compressor	2.5	2	n/a	Yes	-
Scavenging receiver pressure	2.5	2	Yes	Yes	-
Cylinder compression pressure	0.5	5	Yes	Yes	-
Cylinder firing pressure	0.5	5	Yes	Yes	-
Pressure before turbine	2.5	5	n/a	Yes	-
Pressure after turbine	2.5	5	n/a	Yes	-
Temperature after compressor	2	0.9	n/a	Yes	-
Temperature after auxiliary blower	2	0.9	n/a	Yes	-
Temperature after air cooler	0.5	1.4	Yes	No	Input
Temperature at air cooler water inlet	2	0.7	n/a	No	Not used
Cylinder liner wall temperature	0.5	0	Yes	No	Input
Temperature after cylinder	2	4	Yes	No	Not reliable
Temperature before turbine	2	4	Yes	No	Not reliable
Temperature after turbine	2	5.5	n/a	No	Not reliable
Brake specific fuel consumption (BSFC)	n/a	3	n/a	Yes	-

*Calculated indirectly from acquired measurement

It is noted that the engine load is not measured in field conditions. Instead, it is estimated by employing the measured engine speed and fuel injection energizing time along with engine control system (ECS) parameter maps and filters. The estimated load accuracy is adequate in this industrial application, because the ECS controls the engine speed only based on a speed setpoint, so a torque feedback signal is redundant. Additionally, torque meters, require frequent maintenance and recalibration activities.

3.2 Data conditioning

Processing the acquired data, is crucial to ensure reliable reference conditions for both the physics-based model validation and the data-driven model development. The data conditioning approach is developed based on Haben et al. [13] comprising

several pre-processing steps for time-series data. These include data normalization, removal of outlier values, and the final mean value estimation. Data conditioning steps are described in the following paragraphs.

Measured data derived from shop tests do not require any filtering or conditioning, as they are already collected during steady-state engine operating conditions. On the other hand, field measurements are subject to dynamic disturbances, even when the engine speed setpoint is constant, due to the prevailing environmental conditions and ship motions. Performance field operational data conditioning should be conducted prior to any data usage for model development.

By searching within a certain time period (ideally for at least one hour of operation) considering the acceptable engine load change tolerance, the reference stead-state dataset can be identified. Subsequently, the outliers are excluded, and the mean value of this dataset is calculated. The criterion used to identify reference steady state conditions is provided in Eq. (1). This engine load change tolerance is derived empirically from historical performance data analysis of various WinGD engines.

$$|\Delta P_{rel}|\ 100 \leq 1.5\% \qquad (1)$$

Where ΔP_{rel} is the relative engine power or engine load change $(P_{t+1}–P_t)/P_{CMCR}$, whereas P_{CMCR} denotes the CMCR power.

The period being checked is one sampling ratio of 1 minute. Provided that engine load change is well within the accepted tolerance of 1.5% for each sample data point in an one-hour operation, the dataset is stored and prepared for averaging.

The reference steady state conditions are also confirmed by considering an additional criterion according to Eq. (2).

$$|Q1 \bullet [P_{rel} – P_{relMd}]|\ 100 \leq 3\% \qquad (2)$$

This implies that the first quartile (Q1) of the normalized against median value engine load data points of each one-hour window is within a 3% tolerance from the median value. This threshold is also chosen empirically from WinGD Operation Team experts.

A final manual visual inspection is then carried out to ensure that the steady-state conditions determined by using Eq. (1) and Eq. (2) are reasonable. An example of an identified steady-state operating point is shown in Figure 2, where the relative engine load change, as expressed by Eq. (1), is plotted against time. It should be noted that, occasional exceding the tolerance of 1.5% may be acceptable, provided that the rest of the data shows consistent values below the threshold. This is the reason a manual visual inspection is carried out, to avoid eliminating possible steady state cases. Engine load relative to the sample median value is shown on Figure 3.

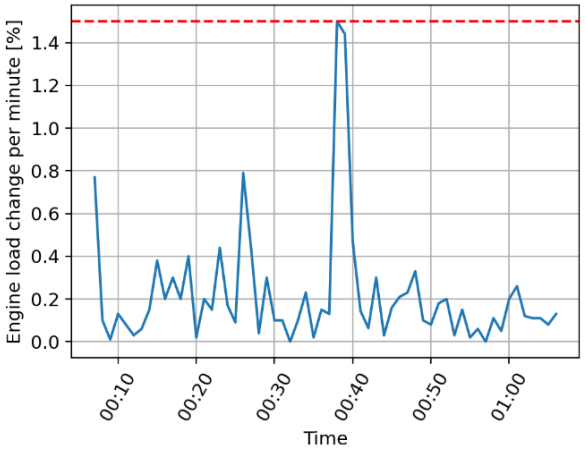

Figure 2. Engine load change on a 1-min basis for 1-hour engine operation that is characterised as steady-state based on Eq. (1).

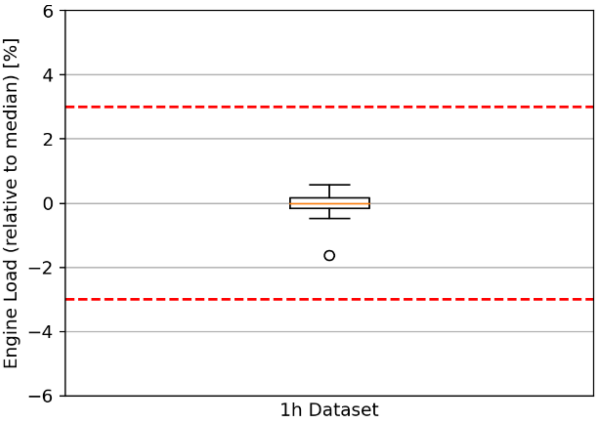

Figure 3. Quartile plot showing engine load subjected from the median dataset value of an 1-hour operation that is characterised as steady-state based on Eq. (2).

In a few datasets, outliers above the 3% threshold were identified for Eq. (2), but since the whisker bars as shown on Figure 3 are well within this limit, the respective datasets are identified as steady state.

Lastly, the analysis of other acquired variables time variations revealed that they follow similar trends as the engine load variation. Hence, this

study clusters the steady-state operation datasets based on the engine load signal.

3.2.1 ISO corrections

Prior to using the measured data, it is essential to correct them at the same reference conditions. All the performance parameters data (measured or simulated) are corrected to standard ISO conditions according to ISO 15550 [14] and ISO 3046 [15]. The ISO corrections are used for a standardised correction of all performance parameters herein.

According to the ISO correction process, the measured pressures and temperatures are corrected empirically considering the reference ambient conditions, scavenging temperature and exhaust backpressures. If a variable is not measured, such as the $\Delta p_{aft.T}$ (backpressure), it is assumed to have the same value as the respective reference value. Reference values are listed in Table 3.

Table 3. ISO reference values

Reference variable	Value	Unit
p_{amb}	1	barA
$\Delta p_{aft.T}$ (CMCR)	300	mmWC
T_{amb}	25	°C
T_{scav} (CMCR)	35	°C
LCV_{diesel}	42,707	kJ/kg
LCV_{gas}	50,000	kJ/kg
$T_{coolant}$	29	°C

Fuel consumption can also be corrected by considering the reference lower calorific value (LCV). However, as LCV is not measured on field conditions, it is not used further than the shop test conversions. More details of fuel LCV data acquisition are found on Section 3.3.4.

3.3 Physics based model

A physics-based model is used to generate artificial data, outside the measured operating envelope, considering both the engine operating point (speed and load) and different fault levels. This model is based on WinGD initial Modular Simulation Platform (MSP), which was developed in the GT-Suite software [16]. The existing model is further customized to accommodate the faulty conditions. The MSP unique characteristic pertains to its modularity, which facilitates to set up new engine models, based on the extensive library of WinGD engine components. Similar modelling approaches have also been used in literature [17]. The layout of the model and the output signals are illustrated in Figure 4. The model is of the physics-based type for most components; however, it includes sub models using data lookup tables. Those components are:

- Turbocharger manufacturer maps for compressor and turbine according to SAE standard.
- Exhaust and wastegate valves, by considering a generic area-depending flow coefficient.
- Auxiliary blower by using its manufacturer map.
- Fuel injectors by using the fuel pressure and injection duration map, that generates fuel flow profiles.

The model is set up for steady-state conditions. This means that the engine speed is provided as input (in the engine crankshaft module), whereas a PID fuel controller adjusts the fuel to achieve the ordered BMEP. The BMEP is estimated by the engine load and speed according to Eq. (4).

$$BMEP = P_{rel} \cdot BMEP_{CMCR} \cdot (N_{CMCR}/N) \quad (4)$$

Where P_{rel} is the engine load (-), $BMEP_{CMCR}$ the rated $BMEP$ (bar), N_{CMCR} the rated engine speed (rpm) and N the engine speed (rpm).

Several signals are not measured on field conditions. Figure 4 illustrates these with orange color. The model was firstly calibrated to match the shop test results corresponding to healthy conditions. The derived results along with their measured values are employed to estimate the pertinent percentage errors. Acceptable error margins are obtained considering the acceptable deviations reported in ISO 15550 [14].

Most of the non-considered signals pertain to temperature measurements of exhaust gas. These measurements exhibit high dynamic variation within each engine cycle, thus rendering the comparison between model and measurement results extremely challenging. Furthermore, field measurements signals with erroneous values were identified, e.g., the temperature after the air cooler. Lastly, other signals such as the EWG opening angle and liner wall temperatures are also not considered for the model validation. The EWG opening is controlled by a PID controller correcting the scavenging pressure to a tuning based setpoint. As the control system model is out of the scope of this study, assessing the opening of the valve seems redundant.

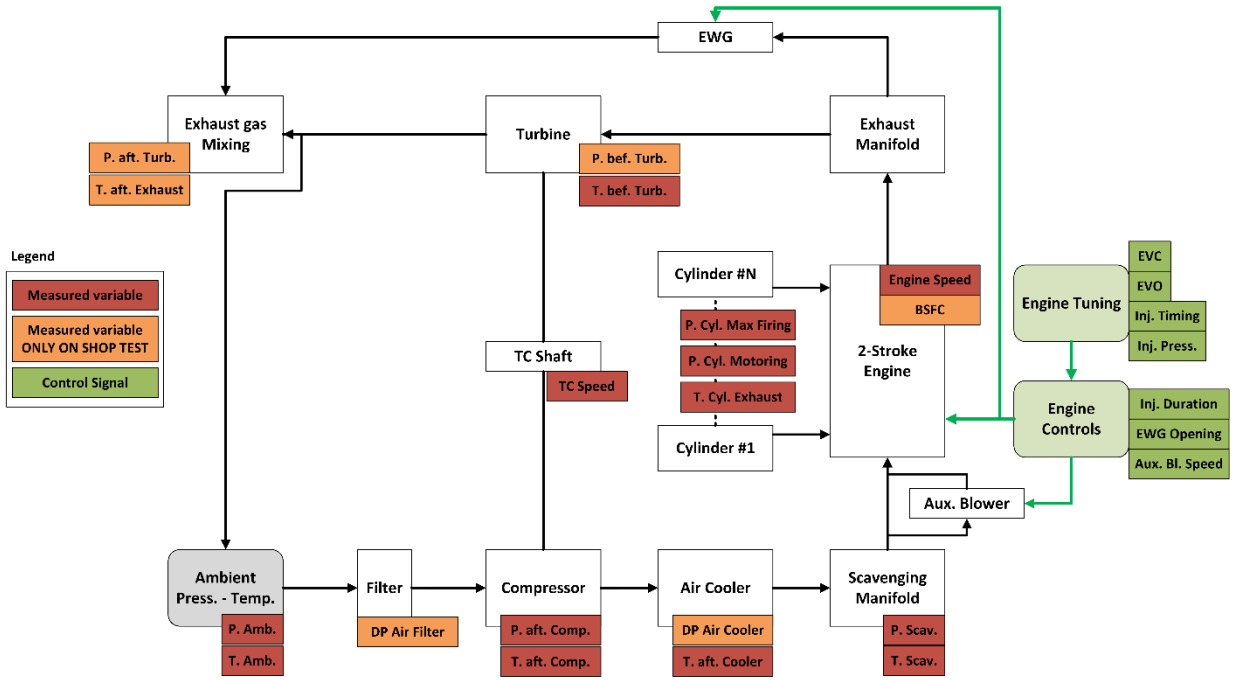

Figure 4. Physics-based model and output signals layout. Red color denotes variables measured during shop tests and field; Orange color denotes variables measured during shop tests; Green color denotes control variables.

Liner wall temperature or cylinder walls temperatures are used as input considering their load dependency. Further details on the main engine sub model systems are provided in the following paragraphs.

3.3.1 Flow model

GT-Suite is a 1D/0D modeling tool, which essentially solves the Navier-Stokes equation [18] for each flow volume, split in three parts for explicit solvers; the conservation of mass, conservation of energy and momentum. The discretization length is chosen in a way to run the model in reasonable computational times, and accuracy to be within the desired levels. Certain components such as air filters and air coolers, where a moderate pressure drop occurs, the discharge coefficient is tuned to match the shop test values at the CMCR point.

3.3.2 Cylinder model

The cylinder model, which is a 0D model, consists of numerous sub models, such as the heat transfer model coupled with a wall temperature template, the combustion model, the scavenging model, the friction model and the input and output flow connections. The input connections regard the air flow through the intake ports and the fuel injection. Exhaust valve is the only component for output flow connections.

3.3.2.1 Heat transfer

The in-cylinder heat transfer model within GT-Suite is the Woschni GT model, which is an adjustment of the well-established Woschni model [19], by eliminating the swirl factor and using one common heat multiplier for all sources. This multiplier is subject to tuning for different loads and speeds.

3.3.2.2 Combustion

For the combustion, the DIPulse object is used, which is the most common template for diesel engines. According to the model designer, the basic approach of this model is to track the fuel as it is injected, evaporates, mixes with surrounding gas, and burns. As such, an accurate injection profile is necessary to achieve meaningful results. This model has been previously calibrated with in-cylinder pressure data of a similar size engine, as there are not available for the investigated system of this project. The fuel injection is performed via already generated profiles, depending on fuel pressure and injection duration. The flow profile is generated using the CFD model for the investigated engine injector. Manufacturer characteristics are taken into account and experimental conditions are applied as input to the CFD model, which in return provides the resulting massflow time profile.

3.3.2.3 Scavenging and friction models

The cylinder scavenging process is modeled with an empirical exhaust residual ratio to a cylinder

residual ratio curve, which is provided as input the GT-Suite.

The friction model used on the engine crankshaft is based on the Chen-Flynn model [20] and is adapted for the WinGD marine two-stroke engines.

3.3.3 Degradation model

The main faulty condition for the injector nozzles, as appeared on numerous field data, is nozzle clogging. The effects of this fault are explored in literature [9], [21] via experimental tests in laboratory conditions on a four-stroke marine diesel engine and simulations. The decreased flow area, the temporally increased fuel injection pressure, and pronounced in-cylinder mixture non-homogeneity [22], [23], [8] cause combustion deficiencies, exhaust gas temperature increase, as well as decreased maximum cylinder pressure, and mean effective pressure.

In order to reflect those symptoms on the DIPulse combustion model, three parameter multipliers are introduced; one for the injector cross-sectional area, one for the combustion efficiency in the form of diffusion combustion rate, and one for the heat transfer accommodating the increased gas temperature. The latter is inversely proportional to wall temperatures, but since wall temperatures are imposed as input in the model, they are being used as tunable parameters depending on the clogging level. From the field data, it cannot be identified if a specific nozzle or injector of a cylinder is defective. As a result, this degradation model represents a whole cylinder, including all fuel injectors. Eq. (5), (6) and (7) show the effects of those mentioned multipliers.

$$\dot{m}_{clog} = C_{clog}\, \dot{m} \tag{5}$$

$$h_{clog} = h\, f_{1,clog} \tag{6}$$

$$C_{df,clog} = C_{df}\, f_{2,clog} \tag{7}$$

Where:

$\dot{m}$ injected massflow rate (kg/s)
C_{clog} injector clog factor (-), 0: fully clogged and 1: healthy
$\dot{m}_{clog}$ injected mass flow rate for clogged injector (kg/s)
h heat transfer multiplier
h_{clog} heat transfer multiplier for clogged injector (-)
$f_{1,clog}$ function adjusting the heat transfer for clogged injector
C_{df} diffusion combustion rate multiplier (-)
$C_{df,clog}$ diffusion combustion rate multiplier for clogged injector (-)
$f_{2,clog}$ function adjusting the diffusion combustion rate for clogged injector

Functions, $f_{1,clog}$ and $f_{2,clog}$, have the role to proportionally adjust the effect of injector clogging on heat transfer and combustion rate respectively. The factors within the function, as well as general heat transfer and combustion rate coefficients, are all calibrated after optimization on both healthy and non-healthy conditions. The considered objective function considers the errors on maximum pressure and compression pressure (simulation against measured values).

3.3.4 Physics based model uncertainties

Despite the physical nature of most of the engine model subsystems, there are uncertainties that remain and could lead to possible inaccuracies or discrepancies. The most significant ones are highlighted herein:

- Unavailability of in-cylinder pressure profiles. The current engine used for the conducted study is not collecting the cylinder pressure profiles, whether in shop test or field conditions. This information would be useful to further tune the engine model to the measured data.
- Scavenging function. The 0D nature of the in-cylinder flow model and the lack of measurement capabilities for trapped masses, makes it practically impossible to validate any scavenging effect with certainty. This may lead to possible deviations on in-cylinder pressures, temperatures and trapped mass.
- Exhaust valve lift profile. The exhaust valves in this engine are solenoid type valves, for which the lift profile is not recorded. Instead, a typical profile for a similar engine has been used, which is derived from the WinGD model library.
- Fuel LCV. For operational field conditions, the engine fuel LCV is not recorded. Even though, fuel analysis reports are available to the authors on a bi-yearly basis, it is not certain if the reported fuel is being used for the next period. As a result, the LCV of fuels is always chosen to have an average value of those reports.
- Engine load measurement. On field conditions, there is no torque meter installed. As a result, the engine load is calculated by combining the engine speed signal, with

empirical and correctional maps of the injection duration. This provides an estimated engine power signal that is used herein.

3.3.5 Physics based model validation

The physics-based model is validated against shop test data and healthy and non-healthy field conditions. Both datasets are subject to ownership of WinGD, and as they are regarded sensitive and confidential information, only normalized and relative information is shown.

The model is assessed based on the maximum value between ISO permissible deviation and sensor error, as expressed on Table 2. The error between model and test data point is calculated according to Eq. (8).

$$u_e = (x_i - \dot{x}_i) / \dot{x}_i \quad (8)$$

Where u_e is the relative error, x_i the model result and $\dot{x}_i$ the test result. All data are compared in SI units.

3.3.5.1 Shop test data validation

The first stage of the model validation is the comparison with shop test data. As previously reported, shop tests are conducted prior to the engine being installed on the vessel, thus results show the most consistent and healthy engine conditions. These shop tests data are final recordings, where the engine tuning is approved to the desired performance criteria, such as power and emissions outputs according to agreements and legislation. Shop test model percentage errors are shown in Table 4.

Table 4. Model to Shop test data relative error for main FPP operating points.

Variable	Percentage error u_e (%)			
Engine load (%)	100	75	50	25
Scav. pressure ISO	0.2	-0.53	-0.03	5.33
TC speed	-0.48	-0.35	-0.71	-7.51
Cyl. Pr. Comp. Mean ISO	0.97	0.03	-0.36	5.35
Cyl. Pr. Fir. Mean ISO	0.34	3.38	-0.41	3.11
DP Air filter	-0.02	-0.12	-0.2	-0.17
DP Air cooler	0.01	-0.13	-0.42	-0.27
Press. Bef. Turbine	-1.15	-2.59	-2.41	5.04
Press. Aft. Turbine	-0.13	-0.19	-0.11	0.13
BSFC ISO	-0.89	0.08	-0.63	-0.09

For in-cylinder variables, only the mean value is shown, because the test showed minimal variation per cylinder. From the results, it is visible that the model has highly acceptable accuracy for most of the load points, except the 25% load. On this operation point, the auxiliary blower is turned on. The blower is a fixed speed compressor, which is modeled via a map-based approach. One uncertainty is that the manufacturer map is referenced to different conditions from what the engine is running. The reference conditions of the blower are 2.2 bar of air pressure and 20°C of air temperature. The air conditions on this operating point on the engine are ~1.6 bar and 15°C. This difference followed by the less accurate turbocharger map on low design speeds [24], reflect on the accuracy of the engine model. Field data review reveals that operation on low loads is frequent, something that impacts the data-driven models accuracy.

3.3.5.2 Field data validation

Field steady state operational data were identified with the approach explained in section 0. The period searched was around 1.5 years of operation, starting from the initialization of digital monitoring systems on the vessel, until the first months of operation upon replacing the investigated components; main fuel injector nozzles. This period range contains both healthy and non-healthy conditions, which depend on the replacement date of the injector nozzles. In total the diesel mode steady-state operating conditions identified were 22 test cases. Out of them, 17 were deemed faulty and the rest 5 of them healthy. These operating points are visible on an engine speed-power map on Figure 5, along with the propeller curve, the maximum limit line and light running margin line. Those three propeller lines are typically defined according to the engine designer [25].

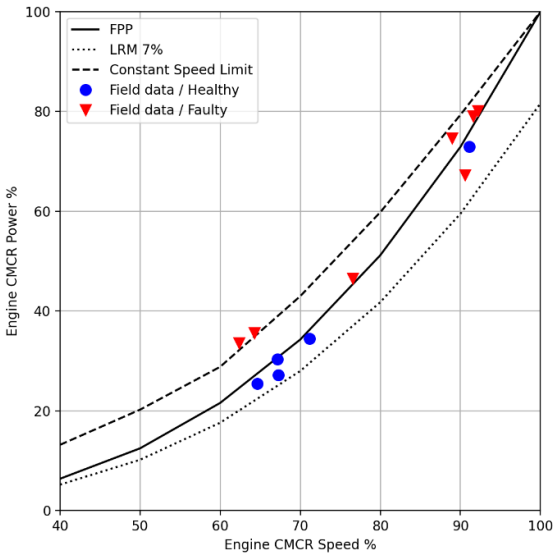

Figure 5. Measured steady-state operating points from the field on the engine load and speed map.

By examining Figure 5, it seems most healthy operating points fall on low load areas, whereas faulty operating points on high engine load areas.

This has a reflection on the engine model validation, because as seen in Table 4, the highest errors appear on the lowest engine load of 25%. The errors of the physics based model on those operating points are visualised in Figure 6 and Figure 7 for healthy and faulty conditions respectively.

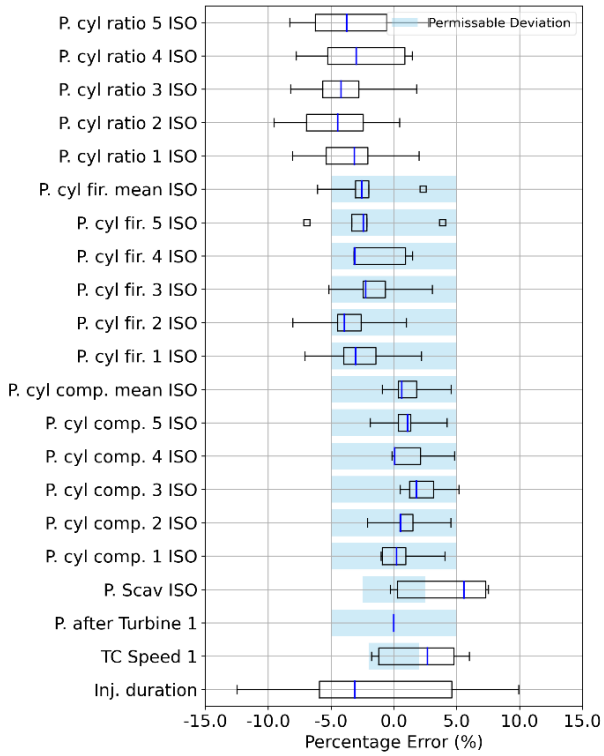

Figure 6. Model error on field measurement for healthy injector nozzle condition.

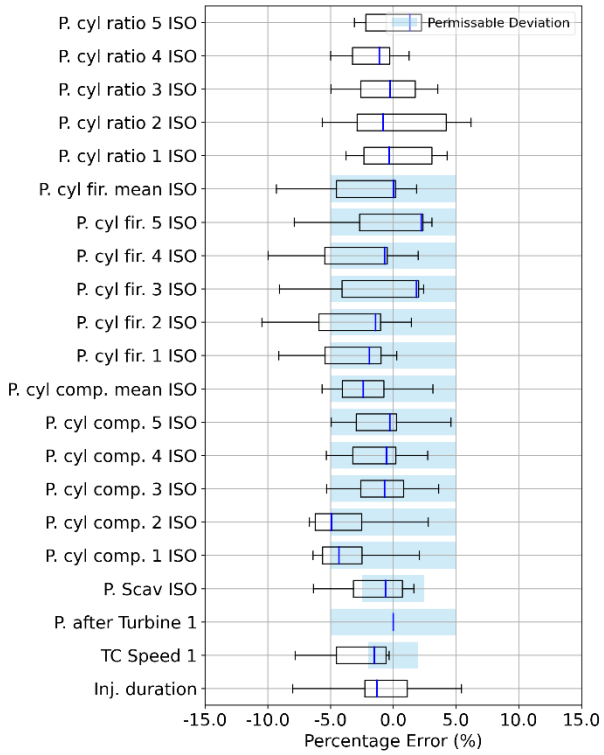

Figure 7. Model error on field measurement for faulty injector nozzle condition.

The two plots show boxplots, indicating the mean error value, the box with the inter-quartile range (IQR) from Q1 to Q3 and whiskers ranging to 1.5 times the IQR distance. Any data beyond the whisker range is deemed as an outlier. The light blue bars show the total uncertainty of the variable from Table 2. *P.cyl. Ratio* refers to the ratio between in-cylinder firing and compression pressure. This is an important variable for field conditions, where the compression and firing pressures do not necessarily have the same level of error. Additionally, as it will be seen on section 3.3.6, it is an important variable for data-driven model training.

Healthy conditions errors are reflecting the model general inaccuracy in low engine loads as expected. This is particularly profound on the injector duration variable. In field conditions, especially at low loads, due to various operating uncertainties, the duration shows a quite high deviation. The causes are not easy to identify, as several boundary and environmental conditions are not monitored, ex. dynamic maneuvering faster than the sampling ratio of recorded data (1 min.), heavy sea, etc. For faulty conditions, as the operating points include both low and high engine loads, the model performs better in terms of accuracy.

The model mean errors for the recorded variables fall within a 5% range, whereas extreme values shown by whiskers range from 5% to 10%.

3.3.6 Extended training and testing data envelope

Upon customizing and validating the physics-based model, which includes individual cylinder injectors fault degradation, a DoE was set up to generate adequate operating points for data-driven diagnostics model training. The DoE consists of 3 main essential parameters alternations: Engine speed, Engine power and the injectors clogging factor. A base speed-load map of points covering most of the operating range is replicated for different levels of injector clogging. The injector clogging factor however is alternating for different levels of degradation on each cylinder individually. The objective is to generate data points to train one cylinder heath index model. This reduces effectively the total number of tests to 6,672 points. The diagnostic application of course is can be applied on each cylinder.

3.4 Data-driven model development

The layout of inputs and outputs of the data driven model for this diagnostic purpose of the study is shown in Figure 8.

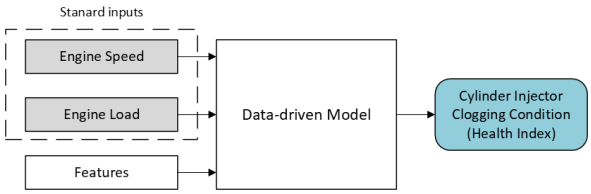

Figure 8. Data-driven model i/o flowchart.

The problem of quantifying the health condition of a clogged injector requires a regression type solution. Among the various data-driven methods found in literature and academic books, most profound for diagnostics and condition monitoring of engines and components are: Deep or Convolutional Neural Networks (NN) [26], [27], [10] k-Nearest Neighbors (kNN) [28], [11] Support Vector Machines (SVM) [12] and linear regression [29]. The advantages and disadvantages of each method are summarised and described in literature [30], [13]. Those four methods are selected for the scope of this project. The steps for the full model development process as described on Figure 1 are:

1. Feature selection
2. Model hyper-parameter tuning
3. Model training
4. Model validation

The data-driven model development is conducted on Python 3.9.12 environment utilizing the most common libraries such as Pandas, Numpy, Matplotlib, Skitlearn and Tensorflow.

3.4.1 Feature selection

Before the training of any data-driven model, the input features with the highest correlation factor should be found and selected. Due to the fairly limited number of measured variables, features which are not so highly correlated are also considered. The Spearman method [31] is selected for feature correlation, as it captures non-linear connections between the features. Table 5 shows the most correlated features. All features are normalization to a [0,1] min-max scale. Excluding the engine load and speed, which are the necessary independent inputs, the highest correlated features include the injection duration compared to healthy shop test values, the injector health condition of the other cylinders, the cylinder pressure ratio, the cylinder compression and maximum pressure, the exhaust gas temperature downstream the cylinder and the scavenging pressure. The ‘Reference FPP’ term refers to the ratio of the signal to the equivalent signal in healthy shop test conditions. Interestingly, several non-measured values such as maximum cylinder temperature, are very highly correlated to the injector fault. Although, most of those variables cannot be measured, they could be acquired with the help of a digital twin model. The exploration of a supportive digital twin on this methodology however, is outside the scope of this study. Lastly, the crankangle of the maximum cylinder pressure is also stated because it is typically offered through fast signal cylinder pressure measurements, however for this engine it was not available.

Table 5. Input features correlation to the injector nozzle clogging factor for cylinder #1.

No.	Feature	Correlation to Inj. Clogging
1	Inj. Dur. Reference FPP	0.47
2	Injector clogg factor Cyl. 2	0.63
3	Injector clogg factor Cyl. 3	0.44
4	Injector clogg factor Cyl. 4	0.28
5	Injector clogg factor Cyl. 5	0.12
6	P. cyl ratio #1	0.43
7	T. After Cyl.Reference FPP #1	0.39
8	P. Cyl. Max Reference FPP #1	0.21
9	P. Cyl. Comp. Reference FPP #1	0.09
10	P. Scav.	0.03
n/a	T. Cyl Max #1	0.89
n/a	Lambda trapped mass #1	0.66
n/a	P. Cyl. Max Crankangle #1	0.08

Afterwards, a parametric analysis is performed between feature no.6-10, to find the optimum number of measured features, by training a data-driven method (kNN) for each number of features. Results of this analysis are illustrated on Figure 9.

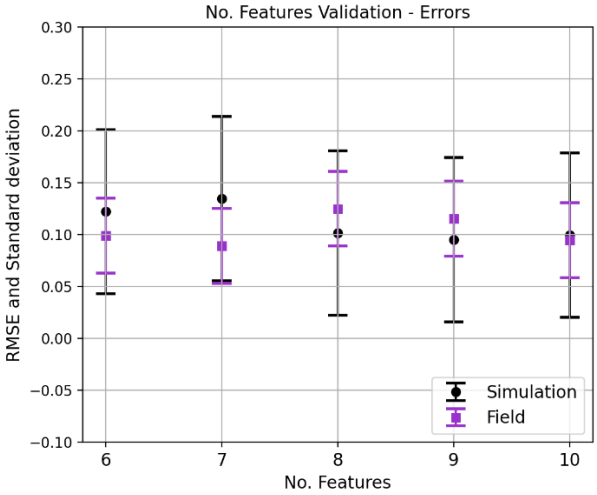

Figure 9. kNN model error to testing data for multiple input features.

The results shown on these plots refer to a 15:85 test-train split of the data of all the simulated dataset (black bars) and the whole field dataset (purple bars). The kNN method used here, is tuned for minimum mean error. Figure 9 shows the RMSE in a whisker bar plot, whereas the 2 standard deviations range is the height of the bar. It is clear from the results that with 9 to 10 features, the error minimizes. That is despite the fact that the last two features have a fairly low correlation factor. For the purposes of examining further the results of the data-driven methodology, 10 features are selected for model training and testing.

3.4.2 Model hyper-parameter tuning and training

Data-driven methods from the four selected ones; MLP, kNN, SVM and linear regression, are having their individual respective hyperparameters tuned for the minimum possible errors and highest R^2 values, in order to find the optimum method for the required task. As an example, MLP is having the number of hidden layers and number of neurons for each layer optimised. This process is done automatically within the Python environment. Each method is then being trained with the same dataset, which consists of 85% of the DoE simulated data. The rest 15% of these data is used for testing the methods.

3.4.3 Model validation

Validation of each method is conducted with simulated data, as well as field test data. The field test data are derived from the same dataset used to tune and calibrate the physics-based model for healthy and faulty conditions, as shown on paragraph 3.3.5.2. The field test data is useful to effectively evaluate the whole methodology in a real-world scenario, albeit a limited one.

3.5 Data-driven model application

The initial purpose of this diagnostic methodology is to apply a per cylinder health index, showcasing the current condition of a chosen component, in this case an injector nozzle. As this application cannot be demonstrated in the framework of this study, because it requires a prepared digital environment on a real vessel, nevertheless the validation and value creation of such a methodology is well illustrated. The final diagnostic model is demonstrated on selected operational data of the investigated engine in Section 4.

4 RESULTS AND DISCUSSION

The outcome of the feature selection showed that most effective number of input features, excluding engine speed and load, is 10. In this Section, the four selected methods are evaluated in terms of performance; namely lowest errors and highest correlation with reference data. Summarized results are shown in Table 6 and Table 7 for simulation and field test data respectively.

Table 6. Data-driven methods errors to Simulated data.

Method	R^2	RMSE	MAPE
MLP	0.86	0.03	0.03
KNN	0.86	0.03	0.02
SVM	0.99	0.01	0.00
Linear Reg.	0.91	0.02	0.02

Results against simulated data show advantage of the SVM methods, however all models show high R^2 and low error values.

Table 7. Data-driven methods errors to Field data.

Method	R^2	RMSE	MAPE
MLP	0.47	0.04	0.03
KNN	-0.37	0.06	0.05
SVM	-1.45	0.08	0.06
Linear Reg.	0.30	0.04	0.03

The method performance on field data on the other hand, shows many differences to simulated data. Here the clear advantage is on the MLP method, as it shows the highest R^2 and lowest errors simultaneously. This interesting result indicates the differences of simulated and real-world testing data regarding data training diagnostic models. A better illustration of those errors for simulated and field data can be seen in Figure 10.

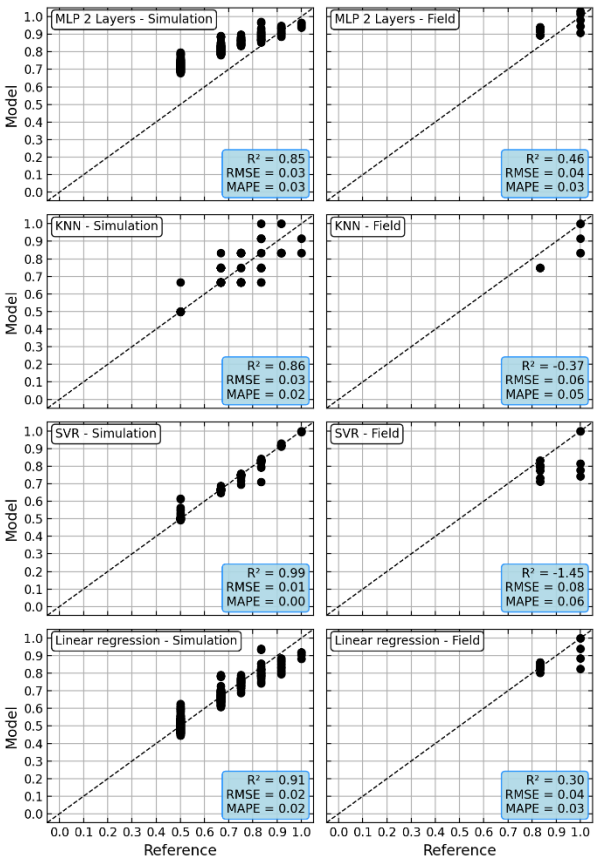

Figure 10. Parity plots for kNN and SVM model results against reference data for 3 input features.

Results show model vs reference data for the clog health condition in a normalized format, where 1 means fully unclogged and 0, the maximum clogged level, as derived from simulations with the criteria being the lowest acceptable burned fuel fraction. The plots show that all models behave similarly for simulated test data, albeit their error differences. Even though the MLP has the lowest R^2 and highest errors for simulated data, for field data the results show the opposite. This makes the MLP model a more robust choice for such purposes. An interesting finding is the satisfactory performance of the simple linear regression model.

For a final step in the model validation on the MLP, validation against test data with the K-Fold cross validation method [32] is also performed. Essentially, the simulated database is split into 5 folds, with each fold containing a 85:15 split of training and testing data. Then each fold is further tested against the same field test data. Results this folded validation are seen on Figure 11.

Judging from the cross-validation results, the MLP model shows solid consistency as RMSE is close to the mean error value across the different folds.

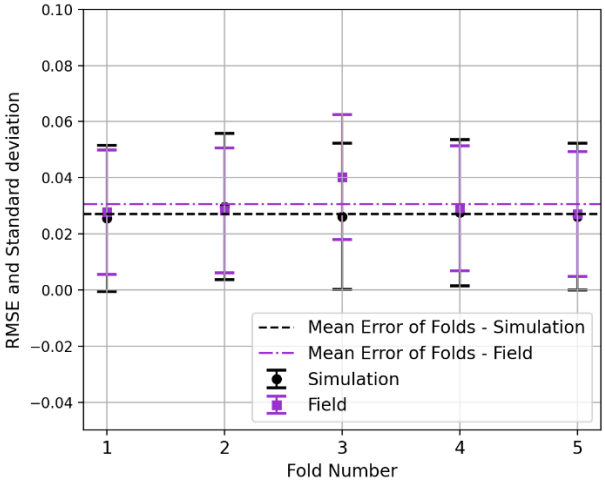

Figure 11. Cross validation for 5 different data folds for KNN model against simulated and field test data.

This ensures that the model training is adequate in predicting a health index of the particular injector nozzles of the investigated system.

5 CONCLUSIONS

This study demonstrated a development methodology for a data-driven approach to diagnose a faulty liquid fuel injector on a marine two-stroke engine. The methodology starts with the utilisation of experimental data in shop tests conditions to tune and customize a physics-based model in GT-Suite environment. Further test data from the operating field conditions, upon conditioning and clustering as healthy or faulty, are incorporated in tuning of a degradation sub-model within the physics-based model. This full engine model is used to generate through a DoE, simulated data for various operating points in several health level conditions of the injector. Finally, a data-driven model is trained and tested through different stages. Results show that the most suitable regression model for this purpose was the MLP NN. The highlighted outcomes are as follows:

- A physics-based model with degradation characteristics is very useful to fill in experimental test gaps and train a data-driven algorithm to various faults. Potential discrepancies of the degradation model and capturing effectiveness of the faults, reflect on the accuracy of the diagnostic methodology.

- Limitations on the number of measured variables pose a barrier on the development of diagnostic algorithms. Several highly correlated variables with the investigated component are not measured. As a result, the full potential of the diagnostic methodology cannot be demonstrated.

- For the investigated system and scenario of clogged injectors, the most suitable data-driven method is the MLP. That is in line with observations of previous studies in literature.

In conclusion, the coupling of data-driven techniques and engine models to the diagnostics of faults within the marine engine environment, show high potential of accurately detecting and isolating the health condition of components. This study results provided confidence in the methods demonstrated, as well pathways for improvement in the areas of the data acquisition and development process. Future studies could further be expanded in multi-variate faults of different components. Finally, predicting the health conditions, will improve condition based and predictive maintenance schemes and such a road path shall certainly build a solid foundation for autonomous shipping in the maritime industry.

6 ABBREVIATIONS & NOMENCLATURE

Abbreviation list

ANN:	Artificial Neural Network
CFD:	Computational Fluid Dynamics
CMCR:	Contracted Maximum Continuous Rating
DoE:	Design of Experiment
ECS:	Engine Control System
EVC:	Exhaust Valve Closing
EVO:	Exhaust Valve Opening
EWG:	Exhaust Wastegate
FPP:	Fixed Pitch Propeller
IMO:	International Maritime Organization
ISO:	International Organization for Standardization
kNN:	k-Nearest Neighbour
LNG:	Liquified Natural Gas
MAPE:	Mean Average Percentage Error
MDO:	Marine Diesel Oil
MLP:	Multi Layer Perceptron
MSP:	Modular Simulation Platform
PID:	Proportional Integral Derivative
PMS:	Planned Maintenance System
SAE:	Society of Automotive Engineers
SVM:	Support Vector Machines
WC:	Water Column
WiDE:	WinGD integrated Digital Expert

Nomenclature list

Amb	Ambient conditions
BMEP:	Brake Mean Effective Pressure (bar)
BSFC:	Brake Specific Fuel Consumption (g/kWh)
P	Power (kW)
Dp:	Delta Pressure (bar)
LCV:	Low Calorific Value (kJ/kg)
RMSE:	Root Mean Squared Error

7 REFERENCES AND BIBLIOGRAPHY

[1] IMO, "2023 IMO STRATEGY ON REDUCTION OF GHG EMISSIONS FROM SHIPS," 2023.

[2] E. Ejder, S. Dinçer and Y. Arslanoglu, "Decarbonization strategies in the maritime industry: An analysis of dual-fuel engine performance and the carbon intensity indicator," *Renewable and Sustainable Energy Reviews,* vol. 200, 2024.

[3] B. J. Georgios Lazaridis Kirolivanos, Comparative reliability analysis and enhancement of marine dual-fuel engines, 2022.

[4] Y. Lv, X. Yang, Y. Li, J. Liu and S. Li, "Fault detection and diagnosis of marine diesel engines: A systematic review," *Ocean Engineering,* vol. 294, 2024.

[5] C. Cartalemi, "A Real Time Comprehensive Analysis of the Main Engine and Ship Data for Creating Value to Ship Operators," CIMAC, 2019.

[6] A. Siegfried, "Service Experience of WinGD's Low-Pressure Dual-Fuel Two-Stroke Engines - The X-DF Engine Generation in the Field," CIMAC, 2019.

[7] WinGD, "X72DF Engine type," WinGD, 2024. [Online]. Available: https://www.wingd.com/en/engines/engine-types/lng-dual-fuel-engines/x72df-1-1/.

[8] J. B. Heywood, Internal Combustion Engine Fundamentals, 2018.

[9] R. Pawletko and S. Polanowski, "Influence of clogged injector nozzles on the heat release characteristics," *Journal of KONES Powertrain and Transport,* vol. 20, 2013.

[10] G. T. Jaehan Jeon, "Datasets envelope impact on marine engines prognostics and health management models accuracy," in *Proceedings of the 33rd European Safety and Reliability Conference (ESREL 2023)*, 2023.

[11] N.-H. Kim, D. An and J.-H. Choi, Prognostics and Health Management of Engineering Systems: An Introduction, Springer, 2017.

[12] A. Coraddu, L. Oneto, D. Ilardi, S. Stoumpos and G. Theotokatos, Marine dual fuel engines monitoring in the wild through weakly supervised data analytics, 2021.

[13] G. T. Jaehan Jeon, A Framework to Assure the Trustworthiness of Physical Model-Based Digital Twins for Marine Engines, 2024.

[14] S. Haben, M. Voss and W. Holderbaum, Core Concepts and Methods in Load Forecasting, 2023.

[15] ISO, 15550:2016, 2016.

[16] ISO, "3046-1:2002," 2002.

[17] A. Palma, I. Sklias, S. Goranov, M. Wenig, E. Serveto and F. Patane, "A Modular Simulation Platform for Rapid and Automated Configuration of 2-Stroke Marine Engine GT-POWER Models," in *EUROPEAN GT TECHNICAL CONFERENCE 2024* , Frankfurt, 2024.

[18] G. Theotokatos, S. Stoumpos, V. Bolbot and E. Boulougouris, "Simulation-based investigation of a marine dual-fuel engine," *Journal of Marine Engineering & Technology,* vol. 19, 2020.

[19] G. Galdi, An Introduction to the Mathematical Theory of the Navier-Stokes equations, Springer, 2011.

[20] G. Woschni, A Universally Applicable Equation for the Instantaneous Heat Transfer Coefficient in the Internal Combustion Engine, 1967.

[21] S. Chen and P. Flynn, "Development of a Single Cylinder Compression Ignition Research Engine," in *National Powerplant and Transportation Meetings*, 1965.

[22] J. Kowalski, "An experimentl study of emission and combustion characteristics of marine diesel engine with fuel injector malfunctions," *Polish Maritime Research,* vol. 189, 2016.

[23] C. D. Rakopoulos and E. G. Giakoumis, "Simulation and analysis of a naturally aspirated IDI diesel engine under transient conditions comprising the effect of various dynamic and thermodynamic parameters," *Energy Conversion and Management,* vol. 39, 1998.

[24] C. D. Rakopoulos and E. G. Giakoumis, "Speed and load effects on the availability balances and irreversibilities production in a multi-cylinder turbocharged diesel engine," *Applied Thermal Engineering,* vol. 17, 1997.

[25] J. Teixeira, O. Sandoval, B. Caetano and J. Baeta, "Turbocharger Performance Prediction: A Review of Map Modelling," *SAE Technical Paper,* 2020.

[26] WinGD, "WX72DF Marine Installation Manual," [Online]. Available: https://www.wingd.com/en/documents/x72df-2-1/engine-installation/mim/marine-installation-manual-(mim)/.

[27] S. Stoumpos and G. Theotokatos, "A novel methodology for marine dual fuel engines sensors diagnostics and health management," *International Journal of Engine Research,* vol. 23, 2021.

[28] H. C. Z. Xiaosheng Li, Research on Remaining Useful Life Prediction of Dual-fuel Main EngineBased on CBAM, 2023.

[29] M. Thurston, M. Sullivan and S. McConky, "Exhaust-gas temperature model and prognostic feature for diesel engines," *Applied Thermal Engineering,* vol. 229, 2023.

[30] P. Odeyar, D. B. Apel, R. Hall, B. Zon and K. Skrzypkowski, A Review of Reliability and Fault Analysis Methods for Heavy Equipment and Their Components Used in Mining, 2022.

[31] C. Croux and C. Dehon, "Influence functions of the Spearman and Kendall correlation measures," *Stat Methods Appl,* vol. 19, 2010.

[32] R. Kohavi, "A Study of Cross-Validation and Bootstrap for Accuracy Estimation and Model Selection," in *International Joint Conference on Artificial Intelligence*, 1995.

8 CONTACT

Mr. Ioannis Sklias
Development Engineer
WinGD Ltd.
Schützenstrasse 3
CH-8400 Winterthur
ioannis.sklias@wingd.com